Effect of UV illumination on perylene-doped luminescent solar concentrators

A cautionary tale

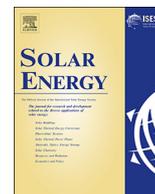Vingerhoets, Lex A.F.; ter Schiphorst, Jeroen; Hagen, Wilfred R.; Debije, Michael G.

Important note
To cite this publication, please use the final published version (if applicable).
Please check the document version above.

Effect of UV illumination on perylene-doped luminescent solar concentrators: A cautionary tale

Lex A.F. Vingerhoets[a], Jeroen ter Schiphorst[b], Wilfred R. Hagen[c], Michael G. Debije[a],*

[a] Laboratory of Stimuli-responsive Functional Materials and Devices, Eindhoven University of Technology, 5600 MB Eindhoven, the Netherlands
[b] Lusoco B.V., 5612 AP Eindhoven, the Netherlands
[c] Department of Biotechnology, Delft University of Technology, 2629 HZ Delft, the Netherlands

ARTICLE INFO

ABSTRACT

The luminescent solar concentrator has the potential of widespread use as a generator of electricity from sunlight well-suited for use in the urban environment owing to its adaptability in shape and coloration. The device performance is heavily dependent on the ability to transport light long distances to the edges. A common organic luminophore used in the device is based on a perylene core. In this work, we describe an overlooked effect of UV illumination on the appearance and efficiency of these devices. An additional absorption peak appears upon polymerization under intense UV in nitrogen atmosphere which significantly reduces the edge emissions from the device. The additional absorbance peak disappears after exposure to air, indicating the presence of a radical anion being formed during the UV light exposure. This suggests newly-produced LSC devices should be allowed to stand a period of time under ambient conditions before their performance characteristics are determined, which could have implications in potential future commercialization of the technology.

1. Introduction

The luminescent solar concentrator (or LSC) is a device allowing generation of electricity from sunlight, and generally consists of a transparent lightguide filled or topped with luminescent molecules for absorbing sunlight and subsequently emitting this light into the light-guiding modes of the plate (Debije and Verbunt, 2012; McKenna and Evans, 2017). Photovoltaic cells (PV) may be placed at the edges of the LSC to be illuminated by the escaping emission light, allowing solar energy generation from sunlight incident to either face of the light-guiding panel, while maintaining the possibility to see through the device. The LSC could complement existing standard silicon-based PV panels, as they may be deployed in areas with prevalence of indirect sunlight (Debije and Rajkumar, 2015), with integration in the built environment eased by their aesthetic possibilities (Kanellis et al., 2016). Other applications of LSCs beyond electrical generation include day-lighting (Earp et al., 2004), greenhouses (Corrado et al., 2016; Sol et al., 2018), and solar chemical reactors (Cambié et al., 2017).

A critical factor in the performance of the LSC device is the ability to transport the dye-emitted light over long distances; this is currently limiting their commercial applicability, as their relative efficiency decreases as the lightguides increase in size. Many factors combine to restrict this transport, including parasitic absorption by the lightguide

material (Kastelijn et al., 2009) and light emitted from the top and bottom surfaces (Debije et al., 2008; Verbunt et al., 2014, 2013), both of which can restrict the potential size and performance of the LSC. However, perhaps of greatest impact is the potential for reabsorption of emitted light during subsequent encounters with embedded dyes as a result of limited Stokes shift of the luminophores.

A very common fluorophore used in studies of the LSC is the perylene-based dye Lumogen F Red 305 from BASF (see Fig. 1a) (Desmet et al., 2012; Seybold and Wagenblast, 1989; Slooff et al., 2008). This dye has proven to have both a high fluorescence quantum yield (FQY) and excellent photostability (Wilson and Richards, 2008). However, in this work we describe the UV-triggered generation of radical anions in Red 305 in LSC devices. The radicals are created in the absence of oxygen during radical polymerization, and remain stable when stored away from air. The generation of additional absorption peaks from these radicals have two major effects on the LSCs. The first is in appearance. The second is more critical, as it has the potential of significantly impacting performance. These radicals are apparently neutralized overnight in the presence of air, suggesting the measurement of the performance of LSC devices employing perylene-based dyes should be delayed a period of time after production if accurate performance values are desired, and placement of these devices in an inert atmosphere (for instance between glass panes in a window), should be
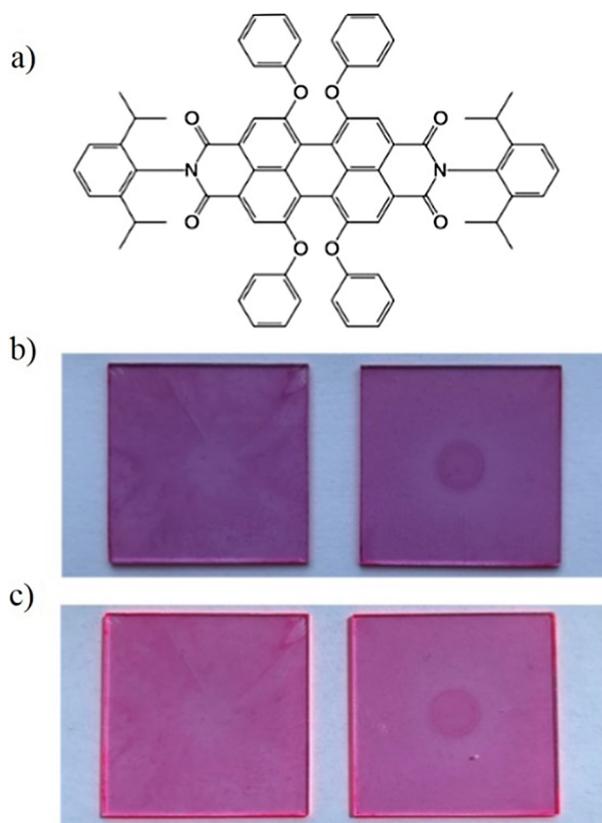
Fig. 1. (a) Structure of Red 305. Photographs of two LSC devices containing 1 wt% Red 305 dye in an acrylate host spin cast on glass lightguides (b) immediately after polymerization under a nitrogen environment, and (c) after exposure to a normal air environment for 48 h. (For interpretation of the references to color in this figure legend, the reader is referred to the web version of this article.)

carefully evaluated. We also provide evidence that these radicals can be generated by prolonged exposure of the panels to intense light, but that these radicals may, too, be 'repaired' over time.

2. Experimental

$3 \times 3 \times 0.1\,cm^3$ glass slides or $5 \times 5 \times 0.5\,cm^3$ PMMA plates (Plano Plastics) were employed as lightguides. A 5:1 wt ratio mixture of dipentaerythritol pentaacrylate (DPPA): methyl methacrylate (MMA) containing 1 wt% Red 305 and 2.5 wt% of the photoinitiators Irgacure 184 and 1 wt% Irgacure 819 (Ciba) was applied to the glass lightguides with a spin speed of 3000 rpm for 30 s. Additional samples were made by bar coating dye solutions via a wire-wrapped bar on PMMA substrates. The resulting glass substrate samples were exposed to UV light from an EXFO Omnicure S2000 lamp at 35 mW/cm² for 10 min (a dose of 21 J/cm²) under a nitrogen atmosphere to polymerize the samples and prevent oxygen inhibition of the radical initiator, or to a Philips tanning light at < 1 mW/cm² UVA for 10 min for samples using PMMA lightguides.

Transmission spectra were measured by a Perkin Elmer Lambda 750 equipped with a 150 mm integrating sphere containing a PMT detector over spectral range of 350–800 nm. To determine the quantum yields and total emission from the sample (edges and faces) the samples were placed inside an integrating sphere ((LMS-100, Labsphere) containing a diode array detector (RPS900, International Light) with a detection range of 350–1000 nm and illuminated through a 0.5 cm circular hole using a 530 nm Thor Labs LED placed outside the sphere. Non-absorbed light was allowed to exit the sphere via a rear aperture. The number of photons absorbed was calculated by measuring the spectral intensity of

the LED and multiplied by the percentage of light that the sample absorbs as determined by UV–Vis spectra (calculated absorbed photons). After UV illumination and measurement, the samples were allowed to sit at ambient conditions in the dark in the laboratory for about 48 h.

Electron paramagnetic resonance spectra were taken on a Bruker EMXplus X-band spectrometer at ambient temperature (20 °C). The modulation frequency was 100 kHz and the modulation amplitude was 4.0 gauss. For the detected radical (see below) microwave power dependence was checked from − 40 to 0 dB (0 dB is 200 mwatt) and the onset of power saturation was found to be near − 30 dB. Therefore spectra were recorded at − 32 dB or 0.126 mwatt.

3. Results and discussion

Photographs of $3 \times 3\,cm^2$ LSC samples on glass containing 1 wt% Lumogen Red 305 (Fig. 1a) in a newly-polymerized acrylate host were taken immediately after removal from the nitrogen box (Fig. 1b) and after sitting at normal atmospheric conditions in the dark for 48 h (see Fig. 1c). There is an obvious difference in the appearances of the two sets of samples: the samples initially appear darker colored with minimal edge emission, but display a much brighter color and significantly more emission after storage in the dark for two days. Additional devices maintained in the nitrogen atmosphere for the period of ~36 h after photopolymerization visually maintained the same darker coloration: after removal from the nitrogen box, the sample converted into the brighter color in a few hours.

To characterize these visual color changes, the transmission spectra of the two samples shown in Fig. 1 were recorded both immediately after polymerization in the nitrogen environment, and after storage at ambient conditions in the lab for 48 h. The results of these measurements are seen in Fig. 2. There is an obvious, broad new absorption peak around 725 nm in the samples after removing from the nitrogen box. The emission spectra from the edge of the lightguides was also recorded, and is shown in Fig. 3.

The fluorescence photon yields (internal efficiency), given by

$$Photon\ Yield = \frac{Emitted\ photons}{Calculated\ absorbed\ photons} \tag{1}$$

from the coatings were estimated from surface and edge emission data for samples placed inside the integrating sphere and exposed to light from a 530 nm green LED, the result of which are seen in Table 1. Thus, while the absorption peak due to the radical anion appears minor in
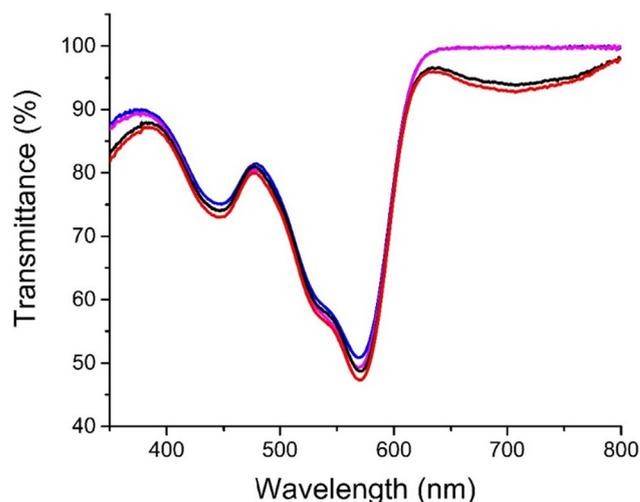

Fig. 2. Transmission spectra of the two LSC devices depicted in Fig. 1 containing 1.0% Red 305 before (black and red lines) and after (blue and magenta lines) exposure to air. (For interpretation of the references to color in this figure legend, the reader is referred to the web version of this article.)
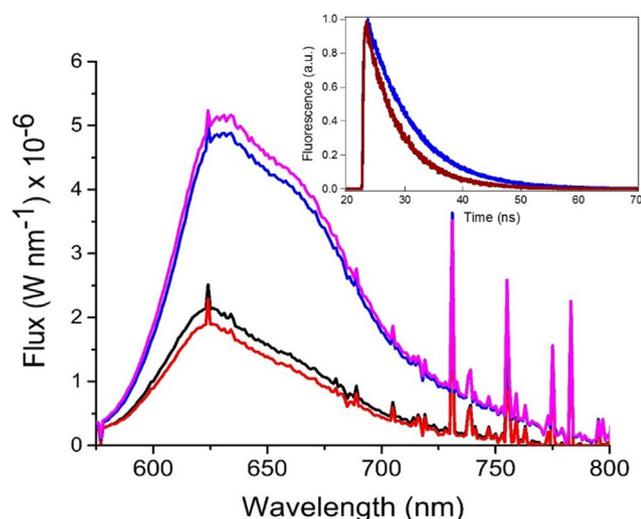
Fig. 3. Emission spectra of the two LSC devices pictured in Fig. 1 before (black and red lines) and after (blue and magenta) exposure to air. Note: the additional sharp peaks above 725 nm are artifacts of the detector and are not the result of the dye emission. (Inset) Fluorescence signal decay for nine year old bar coated sample containing 0.5% Red 305 dye in a photopolymerized acrylate host layer on a PMMA lightguide, both (blue) before and (red) after exposure to high intensity UV light. (For interpretation of the references to color in this figure legend, the reader is referred to the web version of this article.)

Table 1
Estimated photon yield through the edge of the LSC devices based on Red 305 excited by a 530 nm LED source.

Sample	Estimated photon yield	
	Before air exposure	After 48 h air exposure
1	23%	61%
2	19%	62%

transmission, when considering edge emission the impact of reabsorption becomes dominating, and reduces the performance significantly. This additional parasitic absorption would be of even greater impact as the lightguides become larger.

It has been demonstrated previously that perylene dyes in solution can form anionic radical species upon exposure to ultraviolet light (Bhosale et al., 2008; El-Hallag and El-Daly, 2010; Jiao et al., 2015; Perrin and Hudhomme, 2011; Seifert et al., 2015). Some of these radicals show evidence of remarkably long lifetimes (Sharma et al., 2018). These anionic radicals display an additional red-shifted absorption peak with respect to their normal absorbance spectra (Lü et al., 2019; Marcon and Brochsztain, 2007; Schmidt et al., 2015). It is anticipated the radical anion generated during illumination in the nitrogen atmosphere and localized on the perylene-based dye is scavenged by oxygen when the samples are removed to ambient conditions, resulting in a neutral Red 305 molecule and recovery of the anticipated absorption spectra and high emission levels (Shin et al., 2012). Measurements of the fluorescence demonstrated a shortening of the lifetime in the irradiated sample, consistent with the presence of a non-fluorescing radical (see inset Fig. 3).

To verify the presence of a radical species, a $\sim 20 \times 2\,mm^2$ sliver of film was cut from a larger, $\sim 80\,\mu m$ thick film containing 0.2% Red305 and placed inside a quartz tube. Electron paramagnetic resonance (EPR) spectra were measured both before and after exposure to UV light from the same EXFO lamp. The resulting spectra may be seen in Fig. 4. It is quite apparent that before illumination there is no evidence of any radical species, but that there is a clear radical signal after exposure to the UV light.
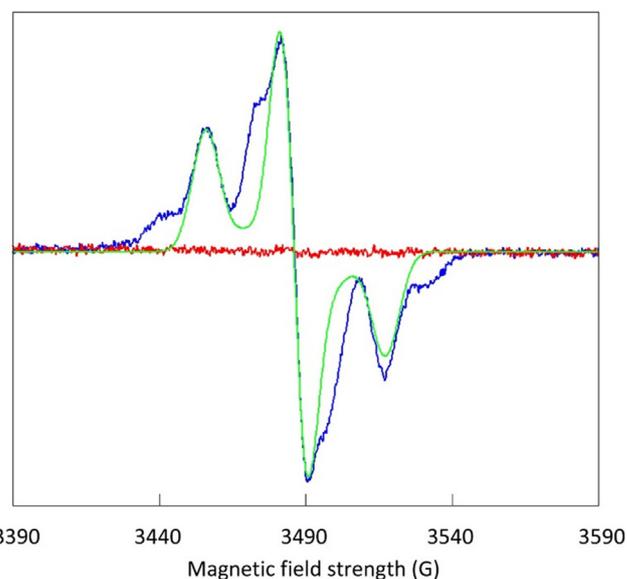

Fig. 4. Electron paramagnetic resonance spectra of 0.2% Red 305 film taken before (red) and after (blue) exposure to UV light for ~ 100 min under nitrogen flow. The microwave frequency was 9780.985 MHz and the non-saturating microwave power was 0.126 mwatt. The green trace is a simulation based on the parameters $g_{zyx} = 2.0042$, 2.005, 2.005; hyperfine spitting $A(^{14}N)_{zyx} = 30.2$, 7, 7 gauss; Gaussian linewidth (half-width-at-half-height) $W_{zyx} = 5.5$, 6.5, 6.5 gauss. The extra shoulders flanking the main spectral features cannot be reproduced with extra ^1H and or ^{14}N splittings; they are ascribed to dipolar interactions. (For interpretation of the references to color in this figure legend, the reader is referred to the web version of this article.)

The gross features of the radical spectrum are highly reminiscent of the well-known EPR from nitroxide spin labels in the rigid limit, (see, e.g.(Goldman et al., 1972)), namely a g matrix with almost unresolved anisotropy and a large nitrogen (I = 1) splitting along the lowest g-value: the radical is nitrogen-based. Additionally, the spectrum exhibits shoulders flanking the three main spectral features. This extra structure cannot be reproduced in simulation with modified g anisotropy in combination with hyperfine splittings from a second nitrogen and/or from one or more protons. We therefore propose its origin to be in dipolar interaction with a second paramagnet, for which a natural candidate would be the second, mirror image N atom in the same Red 305 molecule. In other words, the system is a bi-radical in which mild, through-space dipolar interaction occurs, but in which through-bond exchange interaction between the two S = 1/2 spins is undetectably weak (i.e. the system is not a triplet; indeed, no half-field signal was detected).

To check whether these radicals are only formed immediately after polymerization, experiments on DPPA/1 wt% Red 305 bar coated PMMA devices originally produced 9 years ago and stored in a drawer in the dark were irradiated in nitrogen to a dose of 265 J/cm^2 (at 11.5 mW/cm^2). The samples demonstrated a similar absorbance peak which disappeared after storage in ambient conditions for 2 days (see Fig. 5). These similar results found in experiments on samples both old- and freshly-produced suggest the process of the radical generation is a common one.

There is often a loss of performance between the initial LSC device produced and after extended light exposure due to additional processes leading to degradation of the dye itself (Griffini et al., 2013). Normally, oxygen has been implicated in the degradation of fluorescence in organic dyes (Aitken et al., 2008; Earp et al., 2010; Seybold and Wagenblast, 1989; Slooff et al., 2014), but this work suggests it may also take a part in activation of the device by eliminating specific radical species that reduce the efficiency of emission from the lightguide edges.
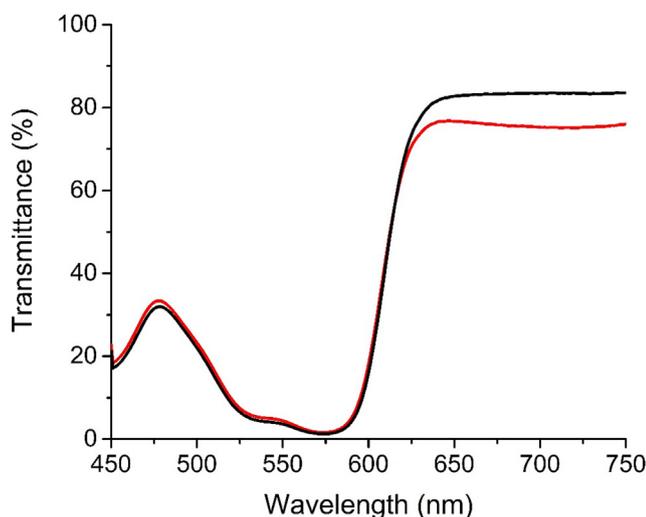
Fig. 5. Transmission spectra of a nine year old bar coated 0.5% Red 305 dye in a photopolymerized acrylate host layer on a PMMA lightguide (black) after exposure to 265 J/cm^2 UV light in a nitrogen atmosphere, and (red) after storage in an ambient atmosphere for two days. (For interpretation of the references to color in this figure legend, the reader is referred to the web version of this article.)

4. Conclusions

We demonstrate the formation of a damage product in perylene-based LSC devices upon irradiation with UV light under a nitrogen atmosphere likely caused by the rapid formation of a radical anion species on the perylene, which persists upon storage away from air. The presence of oxidizing components such as oxygen often is considered as harmful and should be sequestered from the LSC during production and application. However, with the observation that an anionic radical is rapidly oxidized when exposed to air, restoring the performance of the device, a more careful consideration in either expelling oxygen from the device or including new components to prevent the anion formation should be considered. The information contained in this study is of use to workers in the field of LSCs: as the LSC moves towards commercialization, it is important to allow the LSC devices employing perylene-based dyes a period of time after production to recover before measurement of performance characteristics if accurate performance parameters are to be reported. Likewise, daytime performance losses could be 'repaired' during nighttime periods of low illumination.

Acknowledgement

References

Aitken, C.E., Marshall, R.A., Puglisi, J.D., 2008. An oxygen scavenging system for improvement of dye stability in single-molecule fluorescence experiments. Biophys. J. 94, 1826–1835.

Bhosale, S.V., Jani, C.H., Langford, S.J., 2008. Chemistry of naphthalene diimides. Chem. Soc. Rev. 37, 331–342.

Cambié, D., Zhao, F., Hessel, V., Debije, M.G., Noël, T., 2017. A leaf-inspired luminescent solar concentrator for energy-efficient continuous-flow photochemistry. Angew. Chemie 129, 1070–1074.

Corrado, C., Leow, S.W., Osborn, M., Carbone, I., Hellier, K., Short, M., Alers, G., Carter, S.A., 2016. Power generation study of luminescent solar concentrator greenhouse. J.

Renew. Sustain. Energy 8, 1–11.

Debije, M.G., Rajkumar, V.A., 2015. Direct versus indirect illumination of a prototype luminescent solar concentrator. Sol. Energy 122, 334–340.

Debije, M.G., Verbunt, P.P.C., 2012. Thirty years of luminescent solar concentrator research: solar energy for the built environment. Adv. Energy Mater. 2, 12–35.

Debije, M.G., Verbunt, P.P.C., Rowan, B.C., Richards, B.S., Hoeks, T.L., 2008. Measured surface loss from luminescent solar concentrator waveguides. Appl. Opt. 47, 6763–6768.

Desmet, L., Ras, A.J.M.J.M., de Boer, D.K.G., Debije, M.G., 2012. Monocrystalline silicon photovoltaic luminescent solar concentrator with 4.2% power conversion efficiency. Opt. Lett. 37, 3087.

Earp, A.A., Rawling, T., Franklin, J.B., Smith, G.B., 2010. Perylene dye photodegradation due to ketones and singlet oxygen. Dye. Pigm. 84, 59–61.

Earp, A.A., Smith, G.B., Franklin, J., Swift, P.D., 2004. Optimisation of a three-colour luminescent solar concentrator daylighting system. Sol. Energy Mater. Sol. Cells 84, 411–426.

El-Hallag, I.S., El-Daly, S.A., 2010. Photophysical and electrochmical studies of N, N-bis (2,5-di-tert- butylphenyl) -3,4,9,10 perylenebis (dicarboximide) (DBPI). Bull. Korean Chem. Soc. 31, 989–998.

Goldman, S.A., Bruno, G.V., Polnaszek, C.F., Freed, J.H., 1972. An ESR study of anisotropic rotational reorientation and slow tumbling in liquid and frozen media. J. Chem. Phys. 56, 716–735.

Griffini, G., Brambilla, L., Levi, M., Del Zoppo, M., Turri, S., 2013. Photo-degradation of a perylene-based organic luminescent solar concentrator: Molecular aspects and device implications. Sol. Energy Mater. Sol. Cells 111, 41–48.

Jiao, Y., Liu, K., Wang, G., Wang, Y., Zhang, X., 2015. Supramolecular free radicals: near-infrared organic materials with enhanced photothermal conversion. Chem. Sci. 6, 3975–3980.

Kanellis, M., de Jong, M.M., Slooff, L., Debije, M.G., 2016. The solar noise barrier project: 1. Effect of incident light orientation on the performance of a large-scale luminescent solar concentrator noise barrier. Renew. Energy 103, 647–652.

Kastelijn, M.J., Bastiaansen, C.W.M., Debije, M.G., 2009. Influence of waveguide material on light emission in luminescent solar concentrators. Opt. Mater. (Amst.) 31, 1720–1722.

Lü, B., Chen, Y., Li, P., Wang, B., Müllen, K., Yin, M., 2019. Stable radical anions generated from a porous perylenediimide metal-organic framework for boosting near-infrared photothermal conversion. Nat. Commun. 10, 1–8.

Marcon, R.O., Brochsztain, S., 2007. Highly stable 3,4,9,10-perylenediimide radical anions immobilized in robust zirconium phosphonate self-assembled films. Langmuir 23, 11972–11976.

McKenna, B., Evans, R.C., 2017. Towards efficient spectral converters through materials design for luminescent solar devices. Adv. Mater. 29, 1606491.

Perrin, L., Hudhomme, P., 2011. Synthesis, electrochemical and optical absorption properties of new perylene-3,4:9,10-bis(dicarboximide) and perylene-3,4:9,10-bis (benzimidazole) derivatives. Eur. J. Org. Chem. 5427–5440.

Schmidt, D., Son, M., Lim, J.M., Lin, M.J., Krummenacher, I., Braunschweig, H., Kim, D., Würthner, F., 2015. Perylene bisimide radicals and biradicals: synthesis and molecular properties. Angew. Chemie - Int. Ed. 54, 13980–13984.

Seifert, S., Schmidt, D., Würthner, F., 2015. An ambient stable core-substituted perylene bisimide dianion: isolation and single crystal structure analysis. Chem. Sci. 6, 1663–1667.

Seybold, G., Wagenblast, G., 1989. New perylene and violanthrone dyestuffs for fluorescent collectors. Dye. Pigm. 11, 303–317.

Sharma, V., Puthumana, U., Karak, P., Koner, A.L., 2018. Visible-light-triggered generation of ultrastable radical anion from nitro-substituted perylenediimides. J. Org. Chem. 83, 11458–11462.

Shin, I.-S., Hirsch, T., Ehrl, B., Jang, D.-H., Wolfbeis, O.S., Hong, J.-I., 2012. Efficient fluorescence "Turn-On" sensing of dissolved oxygen by electrochemical switching. Anal. Chem. 84, 9163–9168.

Slooff, L.H., Bakker, N.J., Sommeling, P.M., Büchtemann, A., Wedel, A., van Sark, W.G.J.H.M., 2014. Long-term optical stability of fluorescent solar concentrator plates. Phys. Stat. Solidi 211, 1150–1154.

Slooff, L.H., Bende, E.E., Burgers, A.R., Budel, T., Pravettoni, M., Kenny, R.P., Dunlop, E.D., Büchtemann, A., 2008. A luminescent solar concentrator with 7.1% power conversion efficiency. Phys. Stat. Solidi - R 2, 257–259.

Sol, J.A.H.P., Dehm, V., Hecht, R., Würthner, F., Schenning, A.P.H.J., Debije, M.G., 2018. Temperature-responsive luminescent solar concentrators: tuning energy transfer in a liquid crystalline matrix. Angew. Chem. Int. Ed. 57, 1030–1033.

Verbunt, P.P.C., de Jong, T.M., de Boer, D.K.G., Broer, D.J., Debije, M.G., 2014. Anisotropic light emission from aligned luminophores. Eur. Phys. J. Appl. Phys. Appl. Phys. 67, 10201.

Verbunt, P.P.C., Sanchez-Somolinos, C., Broer, D.J., Debije, M.G., 2013. Anisotropic light emissions in luminescent solar concentrators - isotropic systems. Opt. Exp. 21, A485–A493.

Wilson, L.R., Richards, B.S., 2008. High-efficiency dyes for Luminescent Solar Concentrators – photostability and modelling. 23rd European Photovoltaics Conference, Valencia, Spain.